ISSN:2790-1688 Volume-15-(2025)

Interface-Engineered CoFe-Based Phosphide Electrocatalysts Derived from MOFs for Enhanced Hydrogen Evolution Reaction Performance

Jiayi Du

The department of chemistry, University College London, London WC1E 6BT, Britain

zccajdu@ucl.ac.uk

Abstract. The hydrogen evolution reaction (HER) is an efficient and low-cost key half-reaction in water electrolysis that can be a potential way of the long-term sustainable system of hydrogen production in future. In the present work, a well-designed bimetallic CoFe phosphide catalyst prepared by a controlled pyrolysis-phosphorization method was applied to well-designed metal organic structures (MOF) precursor. For improving electrochemical activity of catalyst, carbonization of Fe-doped ZIF-67 by dicyandiamide followed by modification with low temperature phosphidation by NaH2PO2 will be performed. The electrochemical activity of CoFe/HNC-P material is recorded in 1.0 M KOH solution with electrocatalytic activity for HER with an overpotential of 90 mV at 10 mAcm-2 and OER with an overpotential of 313 mV at 50 mAcm-2 with Tafel slopes of 84.7 and 63.0 mVdec-1, respectively. The improved performance is attributed to Fe-induced nucleation of CNTs along with synergetic effect of bimetallic heterointerfaces and hierarchical porosity. XRD shows that codeposited material consists of a mixed phase of phosphide and metal phases well dispersed inside the material, while HRTEM and XPS confirm the existence of well distributed metallic phases inside the material. The real application of our material for water splitting is guaranteed by the terminal performance obtained from the auxiliary information of full-cell water splitting and FEs. The interface-engineering strategy provides a general method to design MOFMOF-based electrocatalysts and apply them as bifunctional catalysts for the water splitting reaction.

Keywords: nanoscale CoFe–Px compounds; catalytic hydrogen evolution process; heterometallic cooperative catalysis.

1. Introduction

Hydrogen, characterized as a clean, renewable, and high–energy-density energy carrier, is regarded as a key enabler in the global transition toward a low-carbon economy and in the pursuit of carbon neutrality.[1] Among the various hydrogen production technologies, electrochemical water splitting has emerged as a promising and environmentally friendly route for scalable, on-demand hydrogen generation. Nevertheless, its practical efficiency is substantially limited by the sluggish kinetics of the hydrogen evolution reaction (HER), especially under alkaline conditions, where the involvement of structured water dissociation media, the additional water dissociation step, and intermediate water adsorption collectively lead to large overpotentials.[2] Therefore, the rational design and development of efficient, durable, and economically viable HER electrocatalysts represents a pivotal step in advancing green hydrogen technologies.[3]Currently, noble metal- and oxide-based materials, especially Pt and its alloys, are widely recognized as benchmark catalysts for the hydrogen evolution reaction (HER), attributed to their near-optimal hydrogen binding energies and minimal kinetic barriers.[4] However, the high cost, scarcity, and inadequate long-term stability of these materials during operation significantly hinder their feasibility for large-scale deployment.[5] In this respect, transition metal (TM)-based materials derived from earth-abundant elements, especially transition metal phosphides (TMPs), have garnered significant interest owing to their distinctive merits, such as excellent electron conductivity, beneficial metal–P bonding characteristics, and inherent structural tunability.[6] Among these candidates, cobalt phosphide (CoP) and iron phosphide (FeP) have exhibited remarkable HER activity in alkaline media. Moreover, the incorporation of two or more metal species (e.g., Co and Fe) into a bimetallic phosphide framework has proven highly effective in enhancing electrocatalytic performance, primarily through synergistic

electronic modulation, active-site heterogeneity, and defect engineering. Despite these advances, a key challenge remains in precisely controlling the composition, morphology, and dispersion of bimetallic phosphides at the nanoscale to fully unlock their intrinsic catalytic potential.[7] In this regard, metal–organic frameworks (MOFs), particularly zeolitic imidazolate frameworks such as ZIF-67, offer an excellent platform for the fabrication of structured and porous electrocatalytic materials. MOFs are distinguished by their homogeneous metal distribution, high surface area, and tunable metal–ligand coordination environments, which can be preserved or modified during thermal conversion. Through rational design, carbonaceous frameworks derived from MOFs can serve as conductive supports that confine active metal species, suppress particle agglomeration, and accelerate charge transport. Notably, Fe^{3+}/ZIF-67 has introduced secondary metal centers for the formation of bimetallic Co–Fe nodes and generated lattice distortions and defect sites during pyrolysis, both of which play a pivotal role in enhancing catalytic performance.[8, 9] Subsequent phosphidation with a phosphorus source such as NaH_2PO_2 yielded CoFeP nanoparticles embedded in hollow nitrogen-doped carbon (HNC), featuring favorable interface structures, abundant accessible active sites, and excellent chemical stability during the hydrogen evolution reaction (HER) under alkaline conditions.[10]

In this work, we present a controllable and scalable synthesis strategy for bimetallic CoFe-based phosphide electrocatalysts (CoFe/HNC-P), using Fe-doped ZIF-67 as the precursor. The material undergoes carbonization under an inert atmosphere followed by low-temperature phosphidation, yielding a hollow spherical structure with uniformly distributed CoFeP nanoparticles. The resulting CoFe/HNC-P catalyst exhibits outstanding HER performance in 1.0 M KOH electrolyte, characterized by low overpotential, a small Tafel slope, and excellent long-term stability. Such superior activity is ascribed to the synergistic effect of Co and Fe, the conductive and porous HNC matrix, and the well-engineered interfaces that facilitate electron transport and optimize hydrogen adsorption–desorption dynamics. This study provides new insights into the rational design of MOF-derived bimetallic electrocatalysts and establishes a general strategy for optimizing electrocatalytic interfaces through heteroatom modulation and structural reconstruction.

2. Experimental procedures

2.1 Experimental materials

All chemical reagents were of analytical quality and used as such. Cobalt nitrate hexahydrate Co (NO3)2·6H2O and Fe (NO3)3·9H2O, 2-methylimidazole, ethanol, deionized water, dicyandiamide C2H4N4, and sodium hypophosphite NaH2PO2 were acquired from Sinopharm Chemical Reagent Co., Ltd. Nitrogen gas with a purity of 99.999% was used as the protective atmosphere, which is utilized during pyrolysis and phosphorization processes, respectively.

2.2 Synthesis routine

2.2.1 Synthesis routine of ZIF-67

Synthesis of ZIF-67 ZIF-67 was prepared by stirring at room temperature of an ethanolic solution of Co(NO3)2·6H2O and 2-methylimidazole. The as-produced purple precipitate was centrifuged and washed three times with ethanol, and then dried under vacuum at 60 degrees Celsius for 12 hours.

2.2.2 Synthesis of CoFe-MOF

In order to prepare the CoFe-MOF precursor, 0.1 g of the as-synthesized ZIF-67 was dispersed by ultrasonication for 10 min in 35 mL of ethanol (Solution A). Separately, 0.05 g Fe(NO3)3*9H2O and 5 ml deionized water under stirring for 5 min (Solution B) were collected. Solution B was then dropwise added into Solution A using vigorous stirring, put under parafilm, and stirred at room temperature for 2 hours. The resulting solid was collected by centrifugation (4000 rpm), washed three times using ethanol, and dried at 60 °C under vacuum for 12 hours to yield the CoFe-MOF in the form of a dark purple powder.

2.2.3 Preparation of CoFe/HNC

For the introduction of a carbon-based framework and intelligence to conductivity, 0.05 grams of the CoFe-MOF was placed in a downstream alumina boat in a tube furnace. A separate, upstream boat containing 0.5 g of dicyandiamide was put upstream. Nitrogen contained in it was removed, and the furnace was heated at the rate of 5 °C min-1 to 700 °C and retained for 2 hours. After natural cooling to room temperature, black powder was obtained, which was designated CoFe/HNC.

2.2.4 Preparation of CoFe/HNC-P

In order to incorporate the P, phosphorion was performed at low temperature. 0.05 g of CoFe/HNC was dosed in one of the boats downstream in the alumina process, and 0.5 g of NaH2PO2. Phosphorus is a chemical element with the symbol P and atomic number 15. 0.5 g of NaH2PO2 was dosed in another boat upstream of CoFe/HNC. In the presence of N2 flow, the furnace was heated up to 320 °C at 2 °C min-1 and was kept for 2 hours. Upon cooling to room temperature, a black powder was obtained as the final product CoFe/HNC-P. CoFe/NC-P (use ZIF-67 as a replacement for CoFe-MOF), control samples such as Co/HNC-P were synthesized using the same conditions for comparison, and CoFe/NC-P (use CoFe-MOF directly without growing carbon nanotube as well).

2.3 Characterization

The morphology and microstructure of the samples were characterized by scanning electron microscopy (SEM) and transmission electron microscopy (TEM). The crystalline phase composition was analyzed by X-ray diffraction (XRD) with Cu Kα radiation (λ = 1.5406 Å). The specific surface area and pore size distribution were determined from N_2 adsorption–desorption isotherms at 77 K using the Brunauer–Emmett–Teller (BET) method. X-ray photoelectron spectroscopy (XPS) was employed to probe the elemental composition and chemical states of Co, Fe, P, N, and C. Additional structural information was obtained from Raman spectroscopy and Fourier transform infrared spectroscopy (FTIR). The electrocatalytic properties toward HER and OER were evaluated using linear sweep voltammetry (LSV), Tafel slope analysis, electrochemical impedance spectroscopy (EIS), and cyclic voltammetry (CV) in a conventional three-electrode setup with 1 M KOH electrolyte. Stability was assessed by chronoamperometry and long-term cycling (CYC) tests.

3. Results and Discussion

3.1 Synthesis Strategy and Morphological Evolution

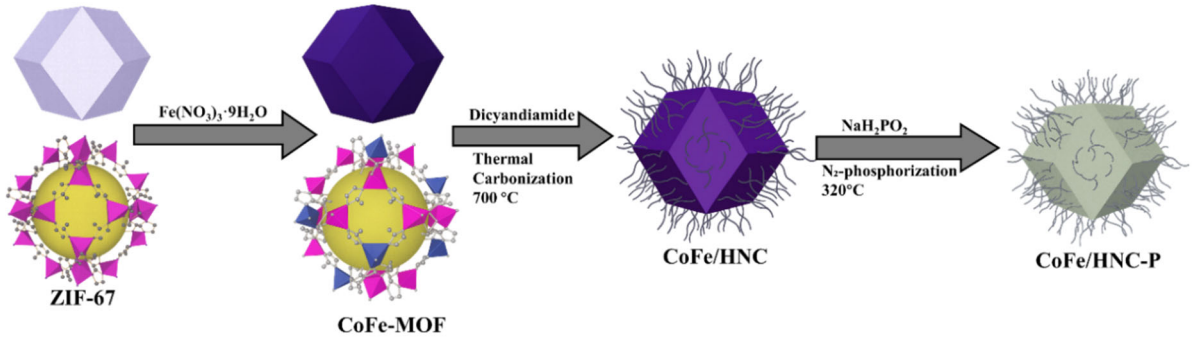

Figure 1 Schematic diagram of formation mechanism of CoFe/HNC-p catalyst.

The synthetic pathway for the CoFe/HNC-P electrocatalyst is schematically illustrated in Figure 1, which outlines the stepwise transformation from the ZIF-67 precursor to the final hollow nitrogen-doped carbon (HNC) framework encapsulating bimetallic phosphides. The zeolitic imidazolate framework ZIF-67 consists of cobalt nodes and 2-methylimidazole ligands which form a rhombic dodecahedral structure with an ordered microporous framework. To introduce bimetallic functionality, Fe^{3+} ions were incorporated through post-synthetic ion exchange or coordination-driven infiltration, yielding a CoFe-MOF with preserved external morphology but modified internal

composition. The incorporation of Fe induces local lattice distortions and generates defect-rich domains within the MOF skeleton, which not only enhance catalytic reactivity but also promote the subsequent nucleation and growth of nanostructures. In the second stage, pyrolytic carbonization was conducted under a nitrogen atmosphere with dicyandiamide serving as an additional carbon source. During this process, the organic linkers decomposed and simultaneously converted into a nitrogen-enriched carbon matrix, while Co and Fe species acted as catalytic centers to trigger the in situ growth of radially aligned carbon nanotubes (CNTs) on the surface of the polyhedral framework. This step resulted in the formation of a distinctive "hairy" morphology, where CNTs emanate from the MOF-derived core, thereby increasing the accessible surface area and providing efficient pathways for charge transport. Subsequent low-temperature phosphidation using NaH_2PO_2 as the phosphorus source produced bimetallic phosphides (CoP and Fe_3P). These phases preferentially nucleated and grew at the CNT tips, on the external surfaces, and within the porous carbon framework. Ultimately, the obtained CoFe/HNC-P structure consists of uniformly distributed CoFeP nanoparticles embedded within a conductive, chemically robust hollow nitrogen-doped carbon matrix. This rationally designed architecture integrates multiple advantageous features: (i) abundant bimetallic active sites from Co and Fe phosphides, (ii) a hierarchical porous framework facilitating mass transport, and (iii) high electronic conductivity arising from CNT networks and the doped carbon matrix. Collectively, these structural attributes underpin the observed improvements in hydrogen evolution reaction (HER) activity and ensure remarkable long-term stability under alkaline electrochemical conditions. Thus, the schematic in Figure 1 provides a conceptual framework that highlights the effectiveness of MOF-derived interface engineering combined with pyrolysis-assisted CNT growth and vapor-phase phosphidation.

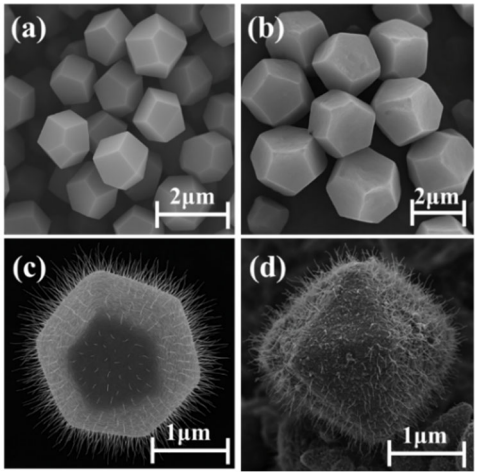

Figure 2 SEM images of morphological evolution for electrocatalysts derived from MOFs during different stages of synthesis: (a) pristine ZIF-67 sample, (b) Fe-doped CoFe-MOF, (c) CoFe/HNC application after pyrolysis with CNT growth, (d) final CoFe/HNC-P application after phosphidation.

The morphological evolution of the catalyst during each critical synthesis stage is clearly demonstrated in the SEM images presented in Figure 2. These sequential micrographs provide direct evidence of the preservation of polyhedral morphology alongside progressive structural modifications induced by Fe doping, carbonization, and phosphidation. Figure 2a displays the pristine ZIF-67 crystals, obtained from the coordination of Co^{2+} ions with 2-methylimidazole in ethanol. The well-defined rhombic dodecahedral particles serve as sacrificial templates for subsequent transformations. After the incorporation of Fe^{3+} via post-synthetic infiltration with $Fe(NO_3)_3$, the resulting CoFe-MOFs (Figure 2b) retain their overall polyhedral morphology and dimensions but exhibit rougher surfaces and sharper facets. These features suggest internal lattice distortions and the formation of defect sites within the framework, which are beneficial for promoting secondary nanostructure growth during thermal treatment. Following pyrolysis under a nitrogen atmosphere in the presence of dicyandiamide, the CoFe/HNC intermediate is obtained (Figure 2c). At this stage, abundant carbon nanotubes (CNTs)

are observed to radially emanate from the polyhedral core, giving rise to a distinctive “hairy” or “urchin-like” architecture. These CNTs, typically hundreds of nanometers in length, significantly increase surface area and establish efficient conductive pathways. Finally, Figure 2d shows the CoFe/HNC-P material obtained after low-temperature phosphidation of the carbonized precursor using NaH_2PO_2 at 320 °C. The polyhedral morphology is largely preserved, while the CNTs remain intact but with roughened surfaces, indicative of the successful nucleation and growth of CoFeP nanoparticles both at the CNT tips and within the carbon framework. Taken together, the SEM analysis confirms that the synthetic strategy ensures morphological conservation coupled with structural transformation at each stage, culminating in the formation of a hierarchical CoFe/HNC-P catalyst. This architecture integrates bimetallic phosphides, conductive CNT networks, and a hollow carbon scaffold, all of which synergistically contribute to the enhanced HER activity and durability under alkaline conditions.

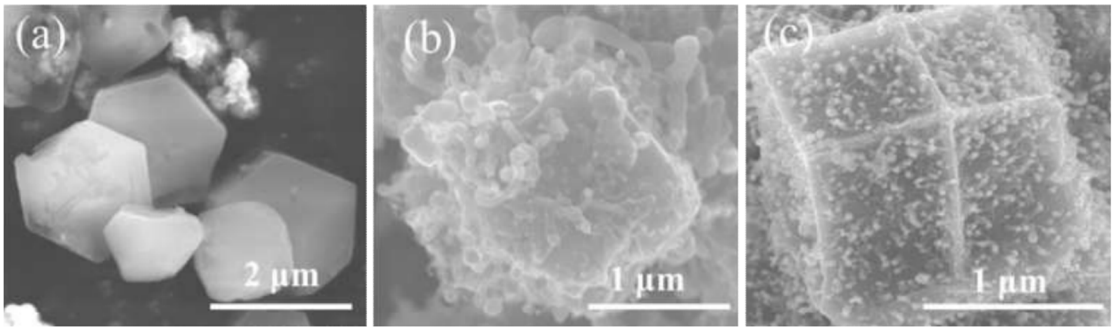

Figure 3 Morphologies of the CoFe/HNC-P sample (SEM images) and its comparison sample under SEM. (a) CoFe/NC-P, (b)Co/HNC-P, (c) CoFe/HNC-P.

Figure 3 displays SEM images of three representative catalysts—CoFe/NC-P, Co/HNC-P, and CoFe/HNC-P—emphasizing structural differences arising from Fe incorporation and CNT growth. These comparative observations provide key insights into the role of Fe incorporation and CNT growth in tailoring the architecture of MOF-derived phosphide electrocatalysts. In Figure 3a, the CoFe/NC-P sample, obtained via direct phosphidation of CoFe-MOFs without CNT introduction, retains a relatively smooth polyhedral morphology resembling its ZIF-67 precursor. Local surface collapse is observed, consistent with stress induced by low-temperature phosphidation. Figure 3b shows the Co/HNC-P catalyst derived from ZIF-67 through pyrolysis in the presence of dicyandiamide, followed by in situ phosphidation. Here, the polyhedral framework is preserved, while randomly distributed CNTs emerge from the surface, decorated with Co nanoparticles. The CNT network increases surface roughness, enhances electrical conductivity, and provides efficient dispersion of catalytic sites. The localization of Co nanoparticles at CNT tips further suggests their catalytic role in CNT nucleation and growth, thereby strengthening the electronic coupling between the conductive carbon matrix and the active sites. Most notably, Figure 3c presents the CoFe/HNC-P catalyst synthesized under identical conditions as Co/HNC-P but with Fe incorporated into the MOF precursor. Compared with the monometallic counterpart, this bimetallic system exhibits CNTs of more uniform length and diameter, homogeneously decorated with ultrafine nanoparticles. The synergistic effect of Co and Fe promotes higher CNT nucleation density, better dispersion of active sites, and improved stability of the polyhedral structure against collapse or sintering. The uniformly aligned CNTs dramatically enlarge the electrochemically active surface area, while simultaneously facilitating charge transport and mass diffusion. Moreover, the intimate contact between metal nanoparticles and the conductive carbon framework forms efficient charge-transfer interfaces, thereby lowering the energy barriers for both hydrogen evolution reaction (HER) and oxygen evolution reaction (OER).

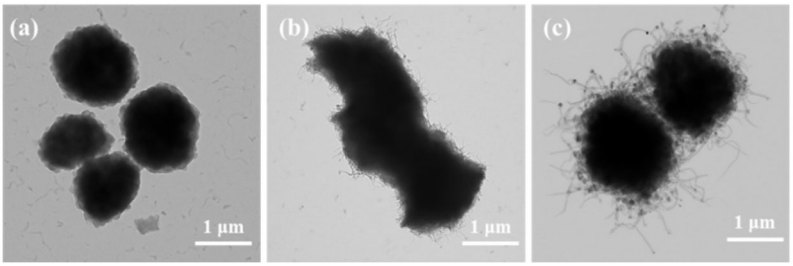

Figure 4 TEM morphology for the CoFe/HNC-P sample and as a comparison sample. So, (a) CoFe/NC-P, (b)Co/HNC-P, and (c) CoFe/HNC-P.

To further probe the nanoscale structures related to electrochemical stability, TEM images of three representative catalysts—CoFe/NC-P, Co/HNC-P, and CoFe/HNC-P—are presented in Figure 4. These images highlight the critical role of Fe incorporation and CNT assembly in constructing conductive frameworks that can mitigate resistance, suppress voltage fluctuations, and enhance long-term durability in electrochemical devices. In Figure 4a, the CoFe/NC-P sample exhibits a hollow polyhedral morphology inherited from its MOF precursor. However, no CNT growth is observed, and the surface remains smooth and compact. The lack of extended conductive networks is expected to hinder charge transport, thereby limiting its electrochemical performance. By contrast, Figure 4b shows the Co/HNC-P sample, in which a limited number of CNTs emerge from the carbon shell. Nevertheless, these CNTs are sparsely distributed, irregular in length and orientation, and poorly interconnected. Such non-uniform features likely compromise mechanical robustness and reduce long-term stability under harsh electrochemical conditions. The optimized morphology is revealed in Figure 4c for CoFe/HNC-P. Here, a dense and periodic distribution of CNTs is observed, with many nanotubes aligned in an organized manner and decorated with well-dispersed metal nanoparticles, either embedded within the carbon matrix or localized at CNT tips. This configuration establishes a robust three-dimensional conductive framework, which simultaneously enlarges the accessible surface area, accelerates electron and mass transport, and maximizes exposure of catalytic sites. Importantly, Fe incorporation into the MOF precursor is found to play a decisive role in regulating CNT nucleation density and uniformity of metal particle distribution. The synergistic effect of Co and Fe not only promotes the controlled growth of CNTs but also strengthens the interfacial coupling between metal phosphides and the carbon framework. Collectively, these nanoscale features provide a structural rationale for the improved activity and durability of CoFe/HNC-P, in agreement with reduced interfacial resistance and enhanced kinetics observed in subsequent electrochemical measurements.

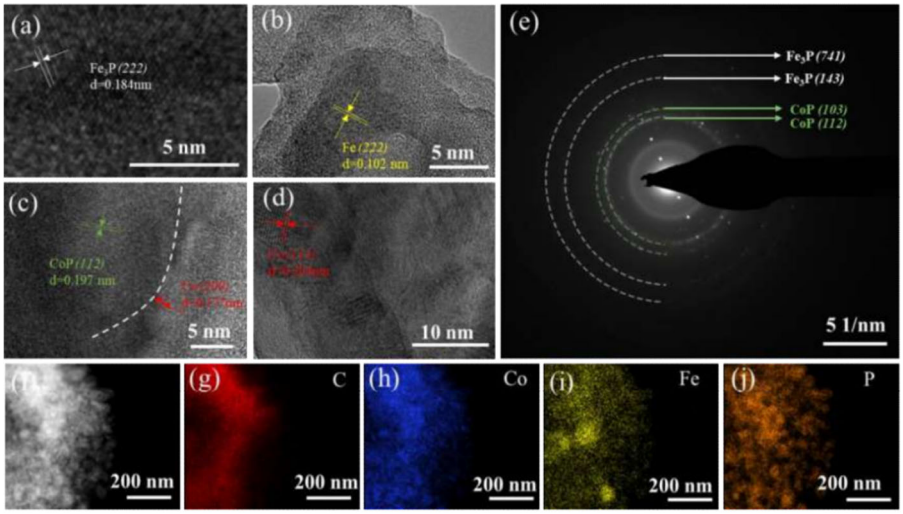

Figure 5 Microstructure of CoFe/HNC-P samples. (a-d) HRTEM images: (e) SAED images; (f) HAADF-STEM images; (g-j) element distribution images.

Figure 5 presents detailed microstructural and compositional analyses of the CoFe/HNC-P catalyst, providing key insights into the correlation between structural features and electrocatalytic

performance. High-resolution TEM (HRTEM) images in Figures 5a–d reveal distinct lattice fringes corresponding to Fe_2P(222), Fe(222), CoP(112), and Co_2P(220) planes, respectively. The coexistence of these multiple phases forms abundant heterointerfaces at the nanoscale, which generate diverse electronic environments and create numerous active sites. The multi-phase heterojunctions show enhanced HER/OER kinetics because of their synergistic effects which are confirmed by subsequent electrochemical data.The selected area electron diffraction (SAED) pattern shown in Figure 5e further confirms the polycrystalline nature of CoFe/HNC-P, with well-defined diffraction rings indexed to Fe_2P and CoP phases. This polycrystallinity provides interconnected grain boundaries that can act as efficient channels for charge transport. The HAADF-STEM image in Figure 5f demonstrates that the metallic nanoparticles are uniformly anchored onto the CNT framework. Elemental mapping (Figures 5g–j) shows homogeneous distribution of C, Co, Fe, and P throughout the carbon matrix, indicating effective incorporation of metal phosphide domains within the conductive carbon network. This uniform dispersion results from the high-temperature phosphidation process, which enables intimate coupling between metallic particles and carbon layers. Importantly, Fe doping not only modulates the electronic structure of the bimetallic phosphide domains but also promotes the nucleation and uniform growth of CNTs. The intimate interfacial contact between metal nanoparticles and conductive carbon further enhances charge transfer efficiency. Collectively, the synergetic contributions from multi-phase heterojunctions, homogeneous element distribution, and hierarchical CNT–carbon scaffolds maximize the electrochemically active surface area while ensuring rapid electron/mass transport and long-term structural stability under operational conditions.

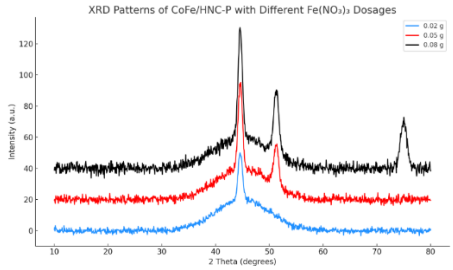

Figure 6 XRD spectra of CoFe/HNC-P materials with various amounts of ferric nitrate added.

Figure 6 shows the X-ray diffraction (XRD) analysis of CoFe/NC-P-HNC composites prepared using various dosages of ferric nitrate (R=0.02 g of alternative aspect HNO3, R=0.05 g of alternative aspect HNO3, and R=0.08 g of alternative aspect HNO3 for sacrificial ZIF-67 = 0.1 g). This experiment was designed to systematically study the influences of different Fe precursor concentrations on the phase composition and crystallinity of the obtained phosphide-based electrocatalysts. From all three samples, characteristic diffraction peaks were detected at 44.9, 65.4, and 82.8 degrees, corresponding to the (110), (200), and (211) planes of metallic Fe (PDF#87-0722). Simultaneously, reflections at 44.4, 51.9, and 75.9 degrees were found as the (111), (200), and (220) planes of metallic Co (PDF#89-7093), as evidence for the pyromagnetic existence of both Fe and Co in their zero valent metallic state. These two phases seem to have a dominating influence on the structure of the crystal observed under all the circumstances we have tested. More importantly, weaker peaks at 40.8 ° and 46.7 ° are attributed to the (002) and (141) planes of Fe3P (PDF#89-2712), whereas the peaks at 31.9 ° and 48.5 ° are ascribed to those at the (011) and (202) planes of CoP (PDF#29-0497). These observations suggest that the occurrence of partial phosphidation of the metallic phases took place during the annealing process, in the presence of a phosphorus source. The presence of both Fe3P and CoP indicates the formation of a hybrid multiphase structure, which is frequently beneficial for electrocatalysis, owing to the presence of several active sites, and to possible electrons arriving on the electronic cooperation at the phase contact interfaces. However, the intensity trends of the diffraction peaks give additional insight into non-competitive phases. As ferric nitrate concentration increased from 0.02 g up to 0.08 g, Fe peak intensity grew significantly and resulted in the suppression of the weaker CoP and Fe3P signal. This suggests that for obtaining a hybrid structure which integrates both metallic and phosphide domains, 0.05 g can be used as the optimal loading amount. Such a structure is anticipated to offer both electron conduction through metallic channels

as well as catalytic behavior from the phosphide interfaces. In summary, as shown in Figure 6, it is important to control the Fe(NO3)3*9H2O content rationally to regulate the crystallographic composition of CoFe/NC-P-HNC materials. The sample containing 0.05 g Fe precursor provides a good combination of active phases, which may contribute directly to increasing electrocatalytic performance for HER or OER reactions.

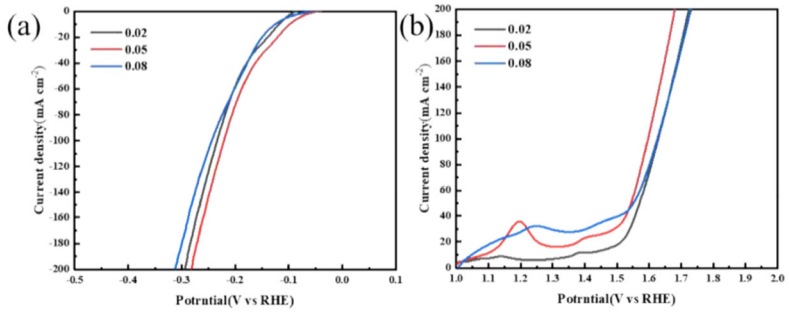

Figure 7 Polarization curves for CoFe/HNC-P prepared by varying amounts of addition of ferric nitrate (a) HER polarization curve|OER polarization curve.

Figure 7 presents the polarization curves of CoFe/HNC-P catalysts with varying $Fe(NO_3)_3$ dosages (0.02 g, 0.05 g, and 0.08 g), evaluated for both hydrogen evolution reaction (HER, panel a) and oxygen evolution reaction (OER, panel b) in 1.0 M KOH electrolyte. This comparison highlights the critical influence of Fe content on the bifunctional electrocatalytic activity of the phosphide-based hybrids. For HER (Figure 7a), all samples exhibit typical cathodic polarization profiles, but the sample synthesized with 0.05 g Fe precursor shows the most favorable performance, characterized by the lowest onset potential and the smallest overpotential required to achieve 10 mA cm^{-2}. These results indicate accelerated reaction kinetics and a reduced energy barrier for hydrogen evolution. By contrast, the catalyst with insufficient Fe content (0.02 g) demonstrates inferior activity, likely due to the limited formation of Fe-based active sites. The 0.08 g sample is intermediate and does not surpass 0.05 g; its deviation is consistent with the compositional trend in Figure 6 (weaker phosphide reflections at higher Fe), suggesting fewer optimally active interfaces. A similar trend is observed for OER (Figure 7b). The 0.05 g Fe sample again exhibits the lowest onset potential and the most rapid increase in anodic current density, indicating enhanced water oxidation kinetics via the four-electron transfer pathway. Moreover, this sample achieves higher current densities at lower overpotentials compared to the other two samples, further confirming its superior bifunctional catalytic behavior. Taken together, these electrochemical results demonstrate that Fe content plays a decisive role in modulating the catalytic interfaces of CoFe/HNC-P materials. Optimal Fe incorporation (0.05 g) promotes the formation of a balanced hybrid structure that integrates abundant active sites with conductive frameworks, thereby enabling superior activity for both HER and OER. These findings underscore the importance of rational precursor engineering in designing transition metal phosphide catalysts for efficient overall water splitting.

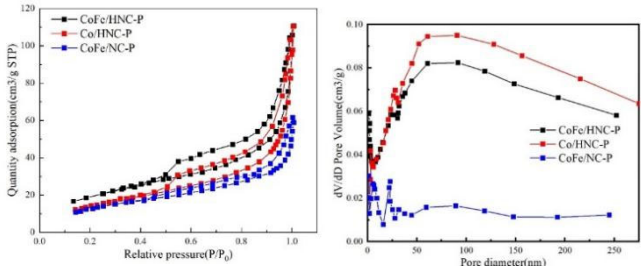

Figure 8 Pore structure characterization of CoFe/HNC-P, CoFe/NC-P, and Co/HNC-P samples. (a) beliefs Temper league; (b) pore size distribution.

To probe the pore structure of the as-prepared catalysts, N_2 adsorption–desorption measurements were performed at 77 K (Fig. 8a). All three samples exhibit type IV isotherms with distinct H_3-type hysteresis loops at relative pressures above 0.8, consistent with slit-like mesoporosity arising from aggregated particles or lamellae.. Among them, Co/HNC-P displays the highest N_2 uptake, followed

by CoFe/HNC-P, whereas CoFe/NC-P shows a considerably lower adsorption capacity. This trend suggests that both Co/HNC-P and CoFe/HNC-P possess relatively high specific surface areas and pore volumes, which are beneficial for exposing active sites and facilitating electrolyte infiltration. By contrast, the markedly reduced uptake of CoFe/NC-P reflects its limited accessible porosity. The BJH pore size distribution profiles (Fig. 8b) further corroborate these findings. Co/HNC-P and CoFe/HNC-P exhibit well-developed mesopores predominantly centered in the range of 20–80 nm, accompanied by a gradual tail extending to the macroporous region, which provides interconnected ion transport pathways. In contrast, CoFe/NC-P shows a much narrower distribution with irregular micropore/mesopore domains and negligible contribution from larger pores, consistent with its suppressed pore volume. Such structural distinctions highlight the critical role of the hollow nanocarbon framework coupled with Fe incorporation and subsequent phosphidation in tuning the porous texture. The synergistic effect endows CoFe/HNC-P with a hierarchically porous structure—balancing mesopore uniformity and macropore accessibility—thereby ensuring efficient mass transport, abundant exposure of catalytically active sites, and ultimately superior electrochemical activity in subsequent catalytic evaluation.

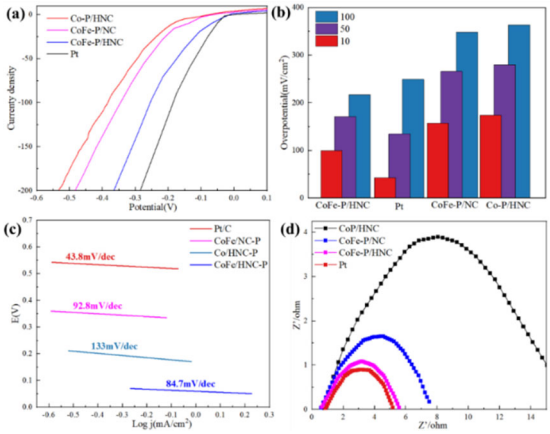

Figure 9 Characterization of the HER catalytic performance of CoFe/HNC-P and comparative samples. (a) LSV for hydrogen evolution curve; (b) overpotentials for 10, 50, 100 mA cm-2 current level; (c) Tafel plot; (d) impedance plot.

The hydrogen evolution reaction (HER) activity of CoFe-P/HNC was systematically evaluated and compared with Co-P/HNC, CoFe-P/NC, and commercial Pt/C. As shown in the LSV curves (Fig. 9a), the overpotential follows CoFe-P/HNC < Co-P/HNC < CoFe-P/NC; at 50 and 100 mA·cm^{-2}, the order becomes CoFe-P/HNC < CoFe-P/NC < Co-P/HNC (smaller overpotential indicates better activity). Overall, CoFe-P/HNC outperforms the other non-noble catalysts across the tested current densities. Quantitative analysis of overpotentials at current densities of 10, 50, and 100 mA cm^{-2} (Fig. 9b) shows that CoFe-P/HNC requires only ≈90, ≈160, and ≈220 mV, respectively, which are markedly lower than those of CoFe-P/NC (≈130, ≈260, ≈340 mV) and Co-P/HNC (≈100, ≈290, ≈360 mV), although still above Pt/C (≈45, ≈120, ≈170 mV). The Tafel slopes (Fig. 9c) further highlight the favorable HER kinetics of CoFe-P/HNC (84.7 mV dec^{-1}), which is smaller than that of CoFe-P/NC (92.8 mV dec^{-1}) and Co-P/HNC (133 mV dec^{-1}), indicating a Volmer–Heyrovský mechanism dominated by the electrochemical desorption step. Moreover, electrochemical impedance spectroscopy (EIS, Fig. 9d) reveals that CoFe-P/HNC possesses a significantly reduced charge transfer resistance compared with Co-P/HNC and CoFe-P/NC, approaching the low resistance of Pt/C, which facilitates faster interfacial electron transport. Taken together, these results demonstrate that the synergistic integration of Fe into the hollow N-doped carbon framework, combined with phosphidation, effectively tailors the porous structure and electronic configuration, thereby reducing kinetic barriers and enhancing catalytic efficiency. Consequently, CoFe-P/HNC emerges as a highly promising non-noble-metal electrocatalyst for practical water splitting applications.

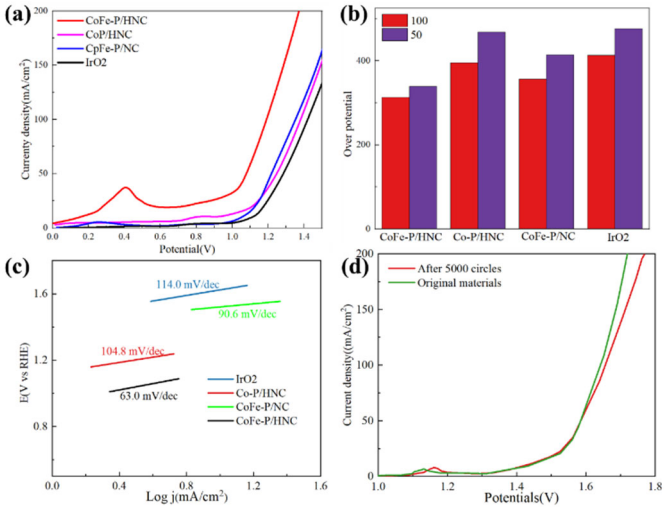

Figure 10 Characterization of the OER catalytic performance of CoFe/HNC-P and comparative sample. (a) LSV curve; (b) Overpotential histogram corresponding to current densities of 50 and 100 mA cm-2; (c) Tafel plot; (d inset) LSV curve of the CoFe/HNC-p sample before and after 5000 cycles; (d inset) V-t curve of CoFe/HNC-p after 40 h of operation at a current density of 50 mA cm-2.

The oxygen evolution reaction (OER) performance of CoFe/HNC-P was systematically assessed and compared with Co/HNC-P, CoFe/NC-P, and IrO_2 (Fig. 10). The LSV curves (Fig. 10a) reveal that CoFe/HNC-P requires the lowest overpotentials among the non-noble-metal catalysts, achieving 313 mV at 50 mA cm^{-2} and 340 mV at 100 mA cm^{-2} (Fig. 10b). These values are markedly lower than those of Co/HNC-P (396 and 466 mV) and CoFe/NC-P (355 and 415 mV), and surpass the performance of of IrO_2 (414 and 474 mV), highlighting the high intrinsic OER activity of CoFe/HNC-P. Tafel slope analysis (Fig. 10c) further demonstrates the favorable kinetics, with CoFe/HNC-P showing the smallest slope (63.0 mV dec^{-1}), which is significantly reduced compared with Co/HNC-P (104.8 mV dec^{-1}), CoFe/NC-P (114.0 mV dec^{-1}), and IrO_2 (90.6 mV dec^{-1}). Durability tests underline the robustness of the catalyst: after 5000 CV cycles, the polarization curve of CoFe/HNC-P exhibits only a minimal shift of ≈20 mV (Fig. 10d), and the chronoamperometric test maintains a stable current density over 40 h at 50 mA cm^{-2}. Taken together, these results indicate that the synergy between Fe incorporation, hierarchical porosity, and phosphidation not only optimizes the active sites and accelerates the reaction kinetics but also ensures long-term durability, establishing CoFe/HNC-P as a highly efficient and stable bifunctional electrocatalyst for overall water splitting.

4. Conclusion

In summary, transition-metal phosphides (TCMs) derived from MOFs have been successfully developed as efficient bifunctional electrocatalysts for overall water splitting. By introducing Fe into a Co-based framework and anchoring the active sites onto a hierarchical nanocarbon matrix, the CoFe/HNC-P catalyst achieves a finely tuned electronic structure, enlarged surface area, and improved electrical conductivity. These synergistic features facilitate rapid charge transfer, enhance electrolyte penetration, and maximize the utilization of active sites. Electrochemical measurements confirm its outstanding catalytic performance: for HER, CoFe/HNC-P requires only 90 mV to deliver 10 mA cm^{-2} with a Tafel slope of 84.7 mV dec^{-1}, while for OER it achieves 50 mA cm^{-2} at 313 mV with a Tafel slope of 63.0 mV dec^{-1}. These values not only surpass those of most control samples but also approach the performance of noble-metal-based catalysts. Moreover, long-term stability tests demonstrate minimal degradation after extended cycling, underscoring the robustness of the hierarchical framework and the reliability of the design strategy. Collectively, this study validates MOF-derived CoFe phosphides as cost-effective, durable, and high-performance bifunctional

catalysts, and provides a rational guideline for the design of advanced non-noble-metal materials toward practical and sustainable hydrogen energy applications.

References

[1] Hanley, E.S., J. Deane, and B.Ó. Gallachóir, The role of hydrogen in low carbon energy futures–A review of existing perspectives. Renewable and Sustainable Energy Reviews, 2018. 82: p. 3027-3045.

[2] Zhu, Y., et al., Alkaline hydrogen evolution reaction electrocatalysts for anion exchange membrane water electrolyzers: progress and perspective. JACS Au, 2024. 4(12): p. 4639-4654.

[3] Zhai, W., et al., Recent progress on the long‐term stability of hydrogen evolution reaction electrocatalysts. InfoMat, 2022. 4(9): p. e12357.

[4] Li, C. and J.-B. Baek, Recent advances in noble metal (Pt, Ru, and Ir)-based electrocatalysts for efficient hydrogen evolution reaction. ACS omega, 2019. 5(1): p. 31-40.

[5] Yang, Y., T. Shen, and X. Xu, Towards the rational design of Pt-based alloy catalysts for the low-temperature water-gas shift reaction: from extended surfaces to single atom alloys. Chemical Science, 2022. 13(21): p. 6385-6396.

[6] Lee, Y., et al., Basics, developments, and strategies of transition metal phosphides toward electrocatalytic water splitting: beyond noble metal catalysts. Journal of Materials Chemistry A, 2024.

[7] Gubóová, A., et al., Bimetallic MoFe phosphide catalysts for the hydrogen evolution reaction. Electrochimica Acta, 2024. 506: p. 145008.

[8] Qian, L.-h., et al., Fe-doped NiCo2S4 catalyst derived from ZIF–67 towards efficient hydrogen evolution reaction. International Journal of Hydrogen Energy, 2022. 47(14): p. 8820-8828.

[9] Zhu, J., et al., Metal–Organic Frameworks Derived Carbon‐Supported Metal Electrocatalysts for Energy‐Related Reduction Reactions. Angewandte Chemie International Edition, 2024. 63(38): p. e202408846.

[10] uang, W., et al., Three-dimensional hollow nitrogen-doped carbon shells enclosed monodisperse CoP nanoparticles for long cycle-life sodium storage. Electrochimica Acta, 2021. 395: p. 139112.